Synthesis and Characterization of a Tertiary Amine Polymer Series from Surface-Grafted Poly(*tert*-butyl acrylate) via Diamine Reactions

Keisha B. Walters*,† and Douglas E. Hirt‡

Dave C. Swalm School of Chemical Engineering, Mississippi State University, Mississippi State, Mississippi 39762-9595, and Department of Chemical and Biomolecular Engineering and Center for Advanced Engineering Fibers and Films, Clemson University, Clemson, South Carolina 29634-0909

Received January 12, 2007

ABSTRACT: A sequence of reaction steps was used to graft poly(*tert*-butyl acrylate) (PtBA) to silicon (Si) wafers and to modify the pendant groups of the tethered PtBA to create chemically tailored surface modifying layers. The Si wafers were first prepared for grafting by the deposition of a self-assembled monolayer (SAM) of *N*-aminopropyldimethylethoxysilane. The terminal primary amine groups on the SAM provided sites for reaction with carboxy-terminated PtBA. The choice of PtBA as the tethered polymer was due to the ability to substitute the *tert*-butyl ester groups with other functionalities. In this study, the *tert*-butyl esters were replaced with various diamines to create a series of polymers with tertiary amine pendant groups. The reactions and surface properties were monitored with external reflectance (ER) and transmission FTIR spectroscopies, ellipsometry, X-ray photoelectron spectroscopy (XPS), and static water contact angle goniometry. Hydrolysis and novel diamine conversion reactions were successfully performed on both neat PtBA homopolymer and end-grafted PtBA (Si-*g*-PtBA). Changes in static water contact angle confirmed the deposition of the *N*-aminopropyldimethylethoxysilane SAM and grafting of the end-functionalized PtBA. Reactions of the surface-grafted PtBA with ethylenediamine and dimethylethylenediamine showed the highest conversion yields.

Introduction

In many biomedical applications, it is important to control the specific chemical functionality at a surface of a device, and many diagnostic and microfluidic devices are currently being constructed on silicon substrates. The use of covalently bound surface layers that can subsequently be modified to give alternate chemistries offers tremendous potential to create tunable surface properties. In addition, the use of covalently bound layers offers more permanence than some other commonly used surface modification techniques (e.g., plasma treatment, corona discharge, adsorption).[1,2]

There has been a significant amount of research on the grafting of end-functionalized polymers on inorganic[3−6] and polymeric[7−9] substrates in the form of films, fibers, particles, or other geometries. In this research, we used silicon wafers to facilitate the characterization of the various reaction steps used to form the surface-grafted layers. The grafted layers were formed from carboxyl-terminated poly(*tert*-butyl acrylate) (PtBA), which is commercially available in various molecular weights with a narrow molecular weight distribution. The PtBA was selected because the pendant *tert*-butyl esters are considered to be good leaving groups and can be replaced with other functional groups. For example, Boyes et al. formed block copolymers from silicon wafers using atom transfer radical polymerization, with one block being PtBA.[10] The *tert*-butyl esters were subsequently converted to acids and then to silver salts. Lee et al. attached an azobenzene alkanethiol to gold to form a brush terminated with *tert*-butyl ester groups.[11] Those terminal groups were then converted to acids using chemical and photochemical methods. In this work, our goal was to investigate a chemical scheme for converting the *tert*-butyl ester pendant groups of PtBA to tertiary amine pendant groups via reaction with diamines. The selection of diamine reactants was due to the ability of tertiary amines to become positively charged at low pH and the potential for reversible changes in polymer conformation, adhesion, separations, wettability, biocompatibility, and more.

Experimental Procedures

Materials. The substrates used in this study were silicon (Si) wafers purchased prediced from Silicon Quest International (N-doped ⟨1,0,0⟩). Carboxy-terminated poly(*tert*-butyl acrylate) (PtBA-COOH) (M_n = 6500, M_w = 7000, M_w/M_n = 1.08) was purchased from Polymer Source, Inc., and used as received. The following chemicals were used as received: dichloromethane (Burdick and Jackson, 99.9+%), 3-aminopropyldimethylethoxysilane (Gelest Inc., >95%), phosphorus pentachloride (Aldrich, 95%), $ZnBr_2$ (Alfa Aesar, 99.9%), sulfuric acid (EMD, ∼91.5%), hydrogen peroxide (VWR, 30%), acetone (VWR, 99.5%), toluene (Fisher, HPLC grade), ethanol (EMD Chemicals, 92%), water (Burdick and Jackson, HPLC grade), and isopropyl alcohol (VWR, 70%). The diamine compounds were purchased from various vendors and were used as received: ethylenediamine (Aldrich, 99%), *N*,*N*-dimethylethylenediamine (TCI America, 99%), *N*,*N*-diethylethylenediamine (TCI America, 98%), *N*,*N*-diisopropylethylenediamine (TCI America, 97%), *N*-isopropylethylenediamine (Aldrich, 98%), and 7-(dimethylamino)heptylamine (Matrix Scientific, 97%).

Monolayer Preparation. Amine-terminated monolayers were prepared on the Si wafers using 3-aminopropyldimethylethoxysilane. The Si wafers were first sonicated for 30 min in isopropyl alcohol and then dried with a nitrogen (N_2) stream. The Si wafers were then treated with a piranha solution (7:3; H_2SO_4:H_2O_2) for 30 min, rinsed thoroughly with water, and then soaked in water for 30 min. The wafers were then dried with N_2 and were ready for the monolayer deposition. The piranha-treated Si wafers were added to a 10 mM solution of 3-aminopropyldimethylethoxysilane in toluene. The samples remained in the silane solution for a minimum of 24 h. The samples were then thoroughly washed and sonicated repeatedly with toluene to remove any adsorbed material, rinsed with ethanol, and dried with N_2.

* Corresponding author: e-mail kwalters@che.msstate.edu, Ph 662-325-7203, Fax 662-325-2482.
† Mississippi State University.
‡ Clemson University.

10.1021/ma0700882 CCC: $37.00
Published on Web 06/13/2007

Grafting of PtBA. *Modification of PtBA-COOH End Group*. The carboxylic acid of the end-functionalized PtBA was converted to acid chloride in preparation for the grafting reaction. To a solution of PtBA-COOH in CH_2Cl_2 a stoichiometric excess of PCl_5 was added. This reaction proceeded with sonication to form the acid chloride end-functionalized PtBA [PtBA-COCl].

Grafting Reaction. The amine-terminated monolayers on Si [Si-NH_2] were then placed into the PtBA-COCl/PCl_5/CH_2Cl_2 solution and allowed to react with sonication to graft the PtBA to Si-NH_2 [Si-*g*-PtBA]. After reaction, the samples were first washed and sonicated repeatedly in CH_2Cl_2. The samples were then rinsed with ethanol and dried with N_2.

***tert*-Butyl Ester Substitution.** Once a layer of PtBA was grafted to the Si surface [Si-*g*-PtBA] using the scheme described above, the pendant *tert*-butyl ester groups were replaced by amine functionalities. The diamines used have the general structure NH_2-$(CH_2)_XNR_1R_2$. While several reaction schemes were evaluated to achieve the *tert*-butyl ester substitution,[12,13] only the results of one are described here. In this study, a saturated $ZnBr_2/CH_2Cl_2$ solution was prepared with stirring for a minimum of 12 h. Aliquots of this $ZnBr_2/CH_2Cl_2$ were added to each Si-*g*-PtBA sample along with the appropriate diamine to form a 0.0045 g/mL solution. These samples were allowed to react for 5 h with sonication.

Characterization. The analysis to monitor the conversion of PtBA-COOH to PtBA-COCl has been documented elsewhere and will not be discussed here.[14] The deposition of the self-assembled monlayer [Si-NH_2], grafting of the PtBA [Si-*g*-PtBA], and conversion of the pendant *tert*-butyl ester groups were monitored using external reflectance (ER) and transmission FTIR spectroscopies, ellipsometry, and static water contact angle goniometry. The ER-FTIR analysis was performed using a Nicolet Nexus 870 instrument and FT-80 horizontal grazing angle accessory with a 80° fixed incidence angle. Transmission FTIR spectra on the silicon wafer samples were obtained using a Thermo-Nicolet Magna 550 FTIR spectrometer equipped with a microscope accessory using a minimum of 32 scans and 4 cm^{-1} resolution. All FTIR characterization was conducted at 25 °C in dry-air-purged chambers. Peak assignments were referenced to literature values.[15−17] Silane and polymer layer thicknesses were analyzed using a Beaglehole picometer ellipsometer. A multilayer model using appropriate *n* and *k* values was fit to variable-angle data to determine the layer thicknesses. Static water contact angle goniometry was used to assess changes in surface wettability. The sessile drop method was used with a Krüss DSA10-Mk2 with digital photoanalysis software. The contact angle values reported are averages of a minimum of nine drops for each sample along with 95% confidence intervals.

Results and Discussion

Amine-Terminated Self-Assembled Monolayers on Silicon Wafers and the Grafting of End-Functionalized PtBA. Silane-based monolayers were chosen over thiol-based monolayers due to the chemical and thermal limitations of the thiol monolayers. For example, heating *n*-alkanethiols adsorbed on gold to 70 °C results in desorption of the thiols and therefore destruction of the monolayer.[18,19] *n*-Alkanethiols have also been found to be sensitive to a variety of chemical agents (including PCl_5).[18,19] This limits the chemical reactions that can be performed with systems built from thiol monolayers on gold substrates. For this reason, alkylsilane monolayers, attached to oxide surfaces via covalent siloxane linkages, were used to give a robust substrate for polymer grafting and substitution reactions. Commercially, there are a limited number of terminal functionalities available on alkylsilane molecules. Of those available, we chose an amine-terminated silane molecule, (3-aminopropyl)-ethoxydimethylsilane (3-APDMES), in order to mimic the chemistry used to graft PtBA to ethylene−acrylic acid films in prior work.[14]

In organic solvents containing some water, the amine group catalyzes the rapid hydrolysis of the ethoxy group.[20] In fact, even traces of water in dried solvents lead to various degrees of hydrolysis and condensation of aminosilane molecules (Figure 1a).[21] Monoethoxysilane was used to limit the formation of oligomers and multilayers from the surface. Two hydrolyzed monoethoxysilanes can form a dimer but will be unable to form a siloxane bond with the surface. The remaining hydroxysilane can either hydrogen bond (Figure 1b) or form a covalent siloxane bond (Si−O−Si) between the hydroxysilane and a hydroxyl group on the silicon surface (Figure 1d).[22,23] For amine-terminated silanes, the amine groups can also hydrogen bond with the surface silanols (Figure 1c). The remaining ethoxy and hydroxyl groups can form hydrogen bonds with the surface silanols and amine groups or form cross-links within the

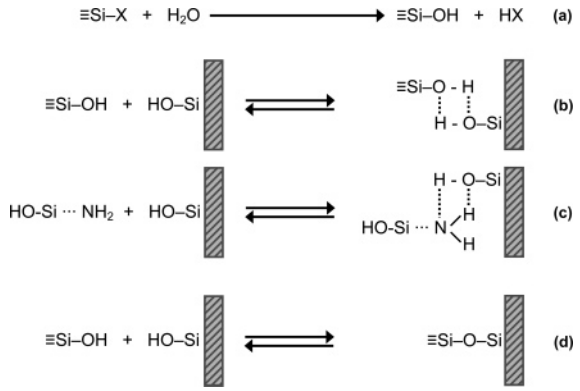

Figure 1. Reaction schemes for silane molecules and the silicon oxide surface: (a) hydrolysis of the silane, (b) hydrogen bonding between the hydrolyzed silane and the silanol groups on the silicon surface, (c) hydrogen bonding between the terminal amine group and the silanol groups on the silicon surface, and (d) formation of a siloxane bond (Si−O−Si) between the hydrolyzed silane and the silanol group. Adapted from ref 24.

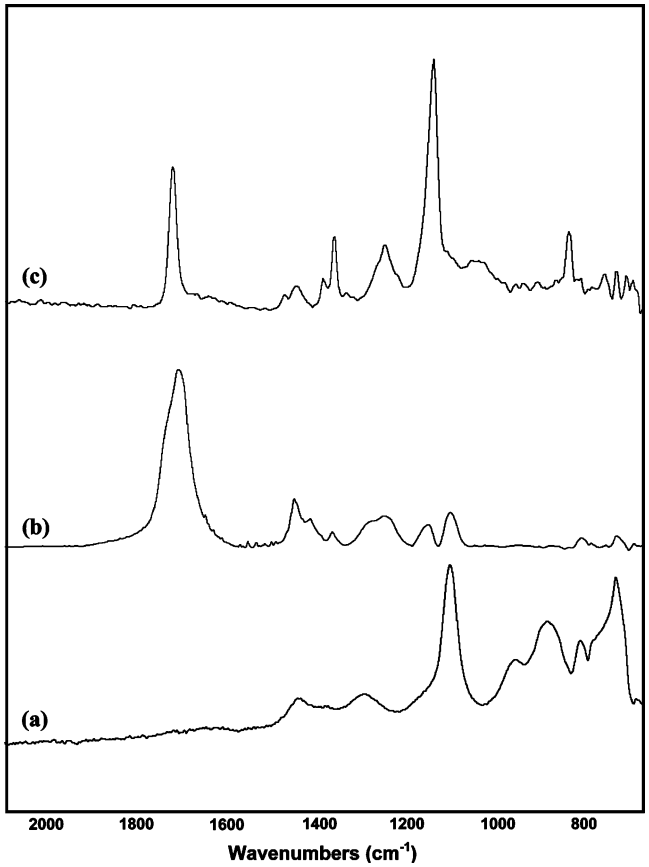

Figure 2. FTIR spectra of (a) Si−NH_2, (b) Si-*g*-PtBA, and (c) neat PtBA.

Table 1. Atomic Composition and Ratios for Si-NH_2 and Si-*g*-PtBA from Survey XPS Scans

sample		experimental	theoretical
Si−NH_2	C	20.1 ± 3.2	41
	O	31.6 ± 0.9	11
	N	2.0 ± 0.6	10
	Si	46.4 ± 3.1	38
	C/N	10.6 ± 2.0	4.1
Si-*g*-PtBA	C	69.5 ± 0.9	72.2
	O	29.9 ± 0.5	27.6
	N	0.6 ± 0.4	0.2

Table 2. Static Water Contact Angle Values from the Literature for Amine-Terminated Monolayers

measured water contact angle (deg)	reference
68−103	44
63 ± 2	43
28−40	21
52 ± 2	26
83.5 ± 1.5	45
63 ± 2	46

coupling layer. The amine groups can also hydrogen bond with the surface hydroxyl groups.[20] Alternatively, in vapor-phase deposition, there is a direct reaction between the silane and surface hydroxyl groups. These reactions generally are performed at high temperatures (>200 °C), which limits the number of available silanes that can be used due to lack of high thermal stability and vapor pressure.[24]

The structure of an amine-terminated silane monolayer can be very complex since there are different attachment modes between the silane and the surface and various possible orientations of the molecule with respect to the surface. The surface coverage and structure are dependent on the reaction parameters including time, temperature, solvent, water content of the solvent, and silane concentration.[21,25] Many researchers have found that amine-terminated silanes usually produce layers with thicknesses greater than the theoretical extended length of the silane (i.e., multilayer structures) and differences in surface density in solution depositions even when dry solvents and environments are used.[19−21,26] Indeed, even though hydroxyl group density on native silicon surfaces is ∼5/nm^2, the measured amine-terminated silane density is shown in the literature to vary widely from 1.5 to 6.4/nm^2.[24,26−28]

Although the propensity of these amine-terminated monolayers to form multilayers has been shown to increase with longer deposition time, the nitrogen content of the resultant monolayers has also been shown to increase.[21] In this work, we are not concerned with producing a well-ordered monolayer. We are simply interested in obtaining terminal amine groups on the layer for subsequent attachment of the end-functionalized polymer. However, while not presented in this work, we did study the effect of varying the environmental condition (N_2 manifold line vs N_2 glovebox), silane concentration (10 vs 100 mM), and deposition time (6, 12, and 24 h). We did not see any significant differences in the thickness or contact angles of the resulting layers due to environment or silane concentration, but we did observe that the layer thicknesses were less consistent from sample-to-sample at higher reaction times (≥24 h). For the rest of this study our layers were prepared using anhydrous toluene and a nitrogen manifold. The average layer thickness for each wafer was measured with ellipsometry and used later in the multilayer model to find the grafted polymer thickness.

FTIR Spectroscopy. ER-FTIR was used to confirm the deposition of the 3-APDMES layer on the silicon wafers (Figure 2a). Peaks were seen at 1445 and 1297 cm^{-1} corresponding to the propyl CH_2 bending and Si−CH_3 deformation, respectively.[29,30] There are two "typical" signature bands for siloxane: a weak absorbance at ∼1870 cm^{-1} for the Si−O combination band and a strong absorbance at ∼1000 cm^{-1} for the asymmetric Si−O−Si stretch.[31−33] The weaker band at ∼1870 cm^{-1} was not seen in our samples. However, the strong band at 1106 cm^{-1} was easily detected. Several bands for the Si−O stretch were also seen at 964, 891, 818, and 738 cm^{-1}.[29,31,32] The higher wavenumber region containing the N−H and C−H stretches was not clear due to distortions in the baseline and difficulties in completely removing water from the purge air. These difficulties were increased for the PtBA grafted samples (Si-*g*-PtBA) since the films are anisotropic and nonmetallic substrates (such as Si) reflect vibrations both parallel and perpendicular to the surface (but in opposite directions) so that the spectra are composed of superimposed upward- and downward-pointing absorptions. Because of this phenomenon, transmission FTIR was performed on the Si-*g*-PtBA samples. (Note that transmission FTIR could not be performed successfully on the Si-NH_2 samples due to the low signal-to-noise ratio.)

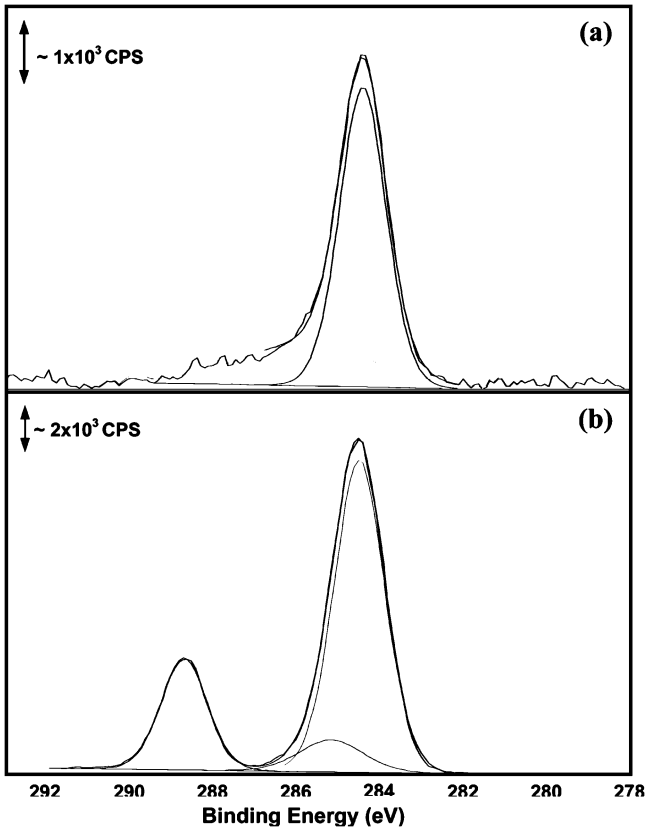

Figure 3. XPS spectra for (a) Si−NH_2 and (b) Si-*g*-PtBA.

A representative transmission FTIR spectrum for Si-*g*-PtBA is shown in Figure 2b. Compared to the ester carbonyl peak at ∼1726 cm^{-1} seen in Figure 2c for neat PtBA, the carbonyl in the Si-*g*-PtBA was shifted slightly to a lower wavenumber (∼1714 cm^{-1}).[29,30,33,34] The shift indicated that some of the *tert*-butyl esters had been converted to carboxylic acids. The carbonyl stretch was also fairly broad and encompassed the absorbance for the amide carbonyl (∼1630−1800 cm^{-1}) that was formed from the grafting of the carboxylic acid end-functionalized PtBA to the amine-terminated layer.[34] The peaks that correspond to the C(CH_3) asymmetric and symmetric stretches were seen at 1478 and 1370 cm^{-1}, respectively, in both the Si-*g*-PtBA and neat PtBA samples.[34,35] The peak at ∼1392 cm^{-1} in both the Si-*g*-PtBA and neat PtBA samples corresponds to the C(CH_3)$_3$ bending deformations.[34] There was

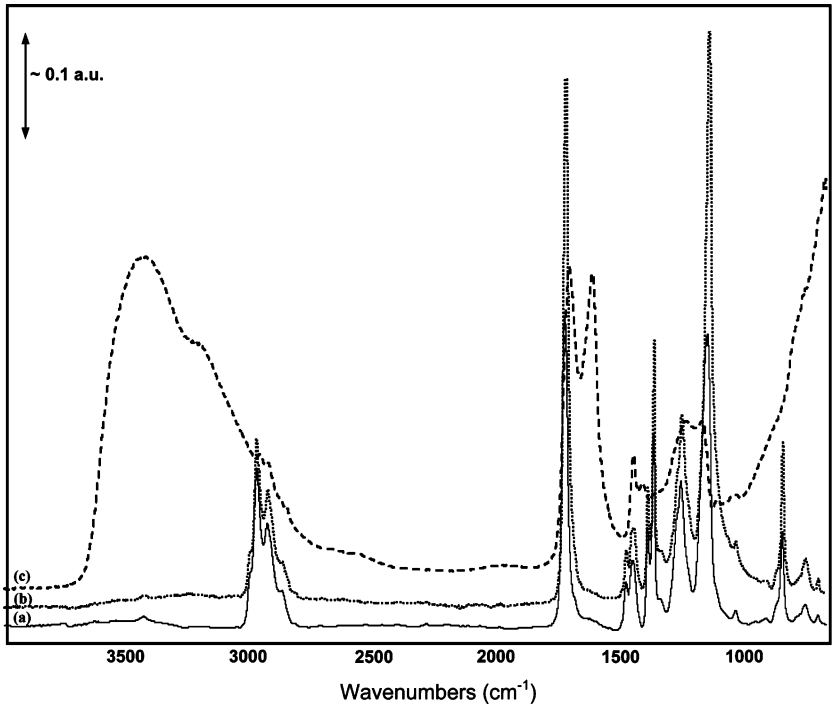

Figure 4. ATR-FTIR spectra for (a) neat PtBA and PtBA homopolymer reacted with sonication and stoichiometric excess of PCl_5 for (b) 30 min and (c) 9.5 h.

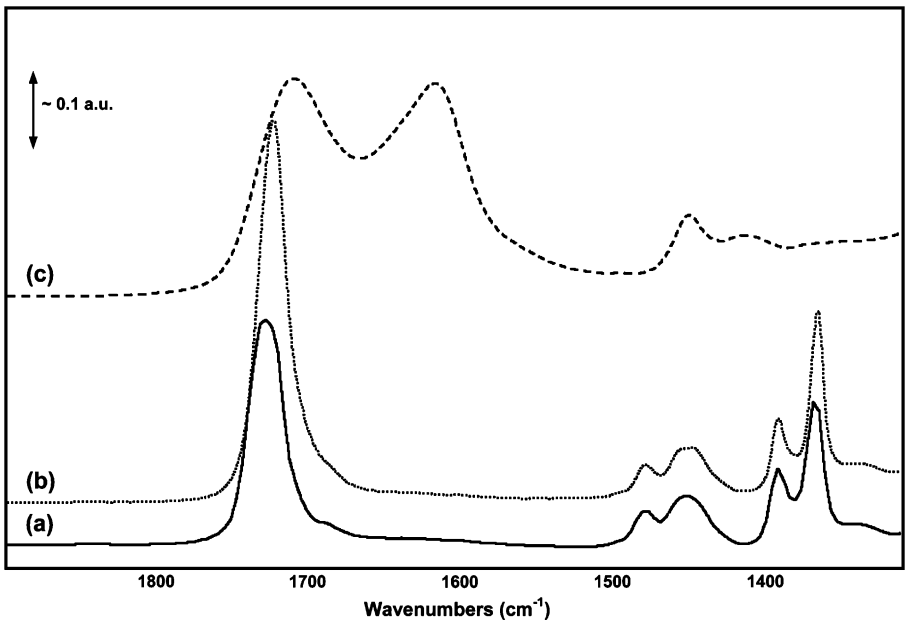

Figure 5. Zoomed-in region of the ATR-FTIR spectra for (a) neat PtBA and PtBA homopolymer reacted with sonication and stoichiometric excess of PCl_5 for (b) 30 min and (c) 9.5 h.

evidence of a peak at ~1290 cm^{-1} in the Si-*g*-PtBA samples which was not present in neat PtBA. This peak corresponds to the amide III absorbance of secondary amides. Both Si-*g*-PtBA and neat PtBA showed fairly strong absorbances at ~1250 cm^{-1} from the skeletal vibration of the $(CH_3)_3CR$ functionality.[34] The C−O asymmetric stretch for ester was found at ~1150 cm^{-1} for both the Si-*g*-PtBA and neat PtBA samples.[29] As expected, this peak was both stronger and broader than the ester carbonyl peak in neat PtBA.[29] Several of the peaks indicative of the silane monolayer were seen in the Si-*g*-PtBA sample including the Si−O−Si asymmetric stretch at ~1106 cm^{-1} and the Si−O stretches at ~818 and 738 cm^{-1}. From these FTIR results, we have been able to confirm qualitatively the deposition of the 3-APDMES layer, grafting reaction of the end-functinalized PtBA, and partial hydrolysis of the grafted PtBA layer. XPS was performed to examine the grafting reactions more quantitatively.

X-ray Photoelectron Spectroscopy. X-ray photoelectron spectroscopy was used to confirm the presence of the amine monolayer and the grafted PtBA on the Si surfaces. Shown in Figure 3 are the high-resolution scans for the Si-NH_2 and Si-*g*-PtBA samples. In both samples, the C−C peak was seen at ~284.5 eV. In the Si-NH_2 sample, the peak at ~286.1 corresponds to C−N.[36−38] After the grafting of PtBA, a strong

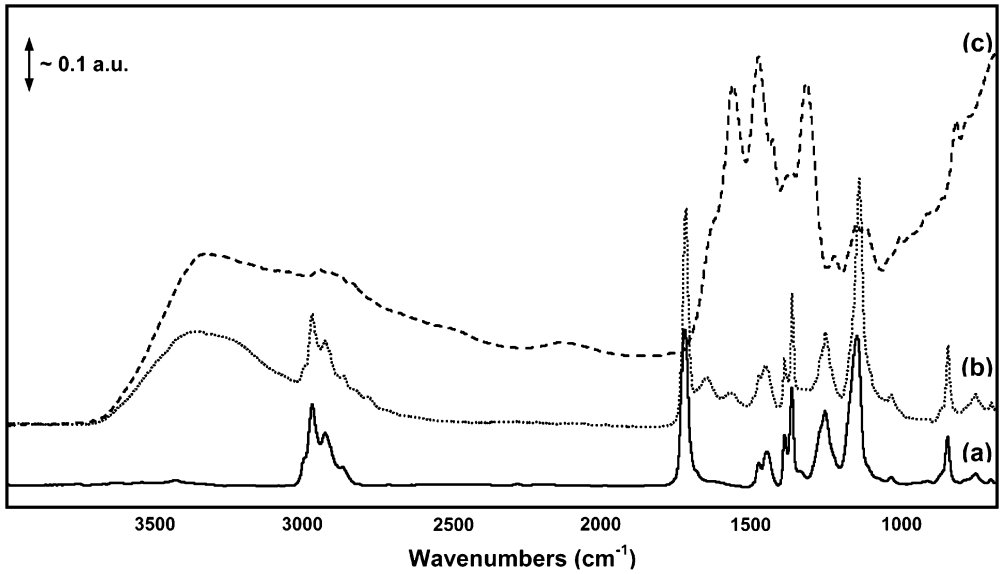

Figure 6. ATR-FTIR spectra for (a) neat PtBA and PtBA homopolymer reacted with dimethylethylenediamine for (b) 2 h and (c) 12 h.

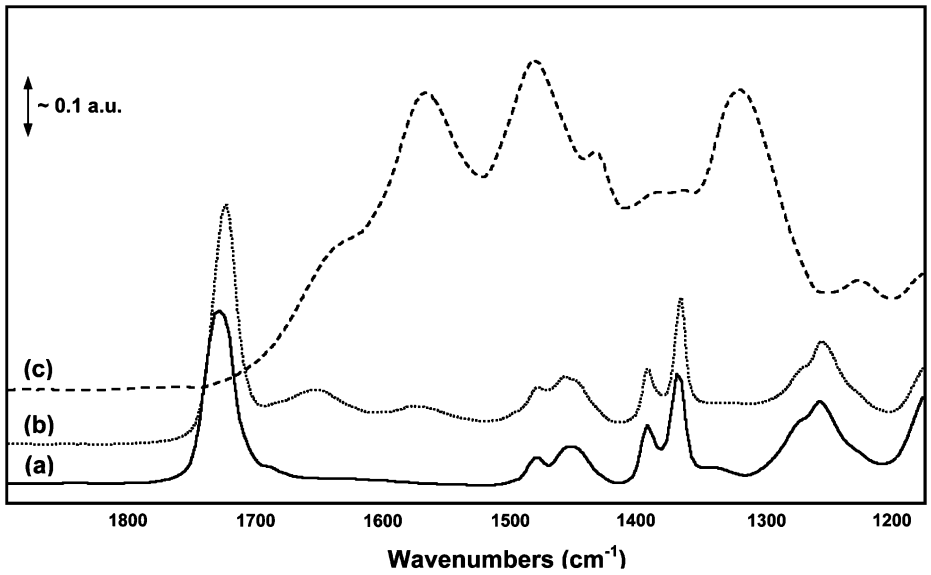

Figure 7. Zoomed-in region of the ATR-FTIR spectra for (a) neat PtBA and PtBA homopolymer reacted with dimethylethylenediamine for (b) 2 h and (c) 12 h.

peak at ∼288.6 eV was seen for the carbonyl carbon (−(*C*═O)O−) in the pendant *tert*-butyl ester groups and possibly includes the carbonyl of the hydrolyzed acid groups (∼289.0 eV).[37,39−41] The peak centered at ∼285.5 eV corresponds to the combination of the *C*−N (∼+0.6 eV), *C*(C═O)N (∼+0.8 eV), *C*−(C═O)O (∼+0.8 eV), (C═O)O*C* (∼+1.2 eV), and *C*$(CH_3)_3$ (*tert*-butyl) (∼+1.7 eV) functionalities.[42]

Table 1 shows the atomic compositions obtained from XPS survey scans of Si-NH_2 and Si-*g*-PtBA. For the Si-NH_2 samples, the C and N atomic percent were lower than theoretical and the O atomic percent was higher, which indicates that the Si surfaces were not completely covered with the amine-terminated silane layer and that there was SiOH remaining on the surface. There is also the possibility that there was adventitious carbon present. For the Si-*g*-PtBA, the experimentally measured values are in reasonable agreement with the calculated values. If nitrogen and Si−O−Si oxygen are neglected (since there would be very few compared to the number of carbons and other oxygens in the grafted layer), the theoretical values would be approximately 72.5% C and 27.5% O. Since the measured C content was lower and the O content higher than the calculated theoretical values, it is likely that some of the *tert*-butyl ester groups were hydrolyzed to acids during the grafting process (theoretical content of poly(acrylic acid) is 53% C and 47% O). Using the measured values of 70% C and 30% O for Si-*g*-PtBA, we estimate that ∼20% of the *tert*-butyl ester groups were hydrolyzed to acids.

Static Contact Angle Goniometry. The static water contact angle of piranha treated Si wafers was ∼0° (the drop completely wetted out). After deposition of the 3-APDMES layer, the static contact angle was 78 ± 0.8°. There is a very wide range of contact angles reported in the literature for amine-terminated monolayers (see Table 2).[21,26,43−46] This makes it difficult to evaluate the structure or density of our layer using contact angle. A change in the contact angle was seen after grafting the PtBA. The contact angle decreased to 62 ± 0.8°, which is lower than the literature value of 75 ± 2° for a grafted PtBA layer[35] but not unexpected since some of the *tert*-butyl ester groups were converted to carboxylic acid functionalities that would lower the water contact angle.

Diamine Conversion Reactions: Control Experiments on PtBA Homopolymer. Prior to carrying out the diamine conver-

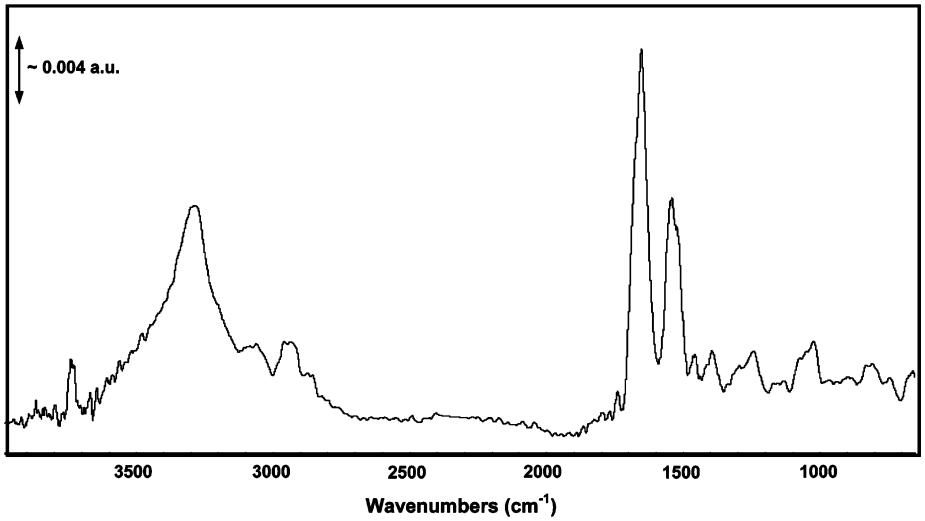

Figure 8. Transmission FTIR of Si-*g*-PtBA conversion with dimethylethylenediamine (Si-*g*-PtBA→DMEDA).

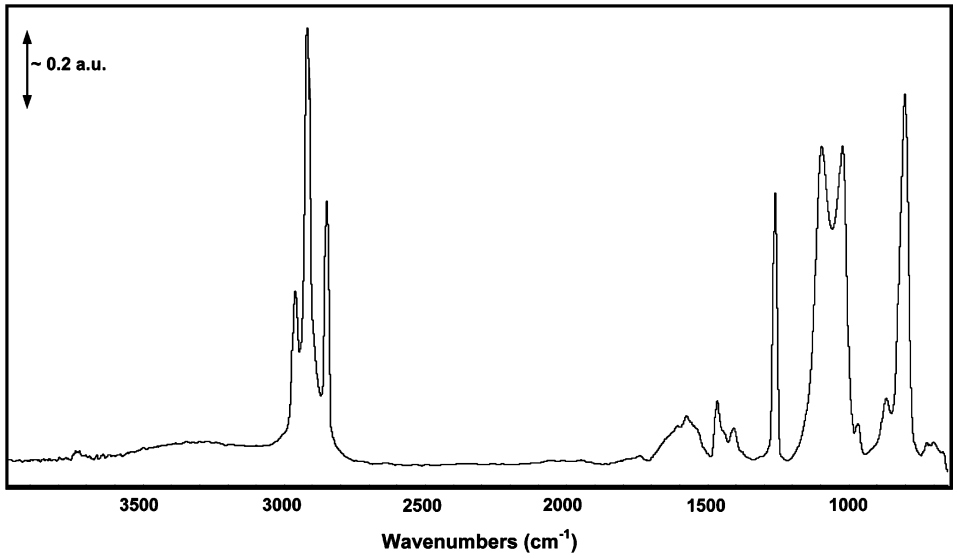

Figure 9. Transmission FTIR of Si-*g*-PtBA conversion with *N*-isopropylethylenediamine (Si-*g*-PtBA→*N*-isoEDA).

sion reactions on the Si-*g*-PtBA samples, several reactions were carried out on PtBA homopolymer. The PtBA was reacted with a stoichiometric excess of PCl_5 in CH_2Cl_2 to convert the polymer into poly(acrylic acid) (PAA). Figure 4 shows ATR-FTIR spectra for neat PtBA and PtBA reacted with sonication for 30 min and 9.5 h. A strong, broad absorption can be seen over the wavenumber range of ∼2700−3700 cm^{-1} for the 9.5 h sample indicative of hydrogen bonding expected in PAA. A closer look at the lower wavenumber region of the spectra is shown in Figure 5. For the 30 min sample, a slight shift of the ester carbonyl (∼1728 cm^{-1}) to ∼1722 cm^{-1} indicated a small amount of conversion of the pendant *tert*-butyl ester groups to acrylic acid. For the 9.5 h sample, the ester carbonyl completely shifted to ∼1709 cm^{-1} (typical band for acid carbonyl). Also, two peaks were seen at ∼1617 and ∼1412 cm^{-1} that are possibly due to the asymmetrical and symmetrical stretches, respectively, of the carboxylate anion, although further study would be required for confirmation.[29,30,34] In the 9.5 h sample, the disappearance of the peaks corresponding to the *tert*-butyl ester groups is apparent. The loss of the $C(CH_3)$ asymmetrical and symmetrical stretch peaks at ∼1478 and ∼1470 cm^{-1} as well as the $C(CH_3)_3$ bending peak at ∼1392 cm^{-1} confirmed the loss of the *tert*-butyl ester groups. Note that this experiment was performed to confirm the potential hydrolysis of the *tert*-butyl groups. A short reaction time of 30 min was used for the conversion of [PtBA-COOH] to [PtBA-COCl] prior to the grafting-to reaction to minimize premature *tert*-butyl hydrolysis.

Similarly, PtBA homopolymer was also used to confirm the diamine conversion reaction. In Figure 6, the ATR-FTIR spectra are shown for neat PtBA and PtBA that was reacted with dimethylethylenediamine (DMEDA) for 2 and 12 h using the $ZnBr_2$ procedure described previously. A broad absorbance can be seen in both reacted samples at high wavenumbers, composed of N−H stretching that is centered at ∼3300 cm^{-1} and the amide B band (first overtone of the amide II band) at ∼3100 cm^{-1}.[29,30,34,46−48] The peak for the 12 h sample, however, is especially broad, which may be due to hydrogen bonding between the amide and amine groups of adjacent pendant groups.[29,49] As can be seen in Figure 7, further evidence of the *tert*-butyl ester to diamine conversion is shown by the slight shift in the ester carbonyl peak between neat PtBA (∼1728 cm^{-1}) and the 2 h sample (∼1722 cm^{-1}) and the complete disappearance of the ester carbonyl in the 12 h sample. The amide I band (C−O and C−N stretches) can be seen at ∼1652 cm^{-1} for the 2 h sample and at ∼1628 cm^{-1} for the 12 h sample. The difference in absorbance of the amide I band between these two samples may be explained by the hydrogen bonding seen

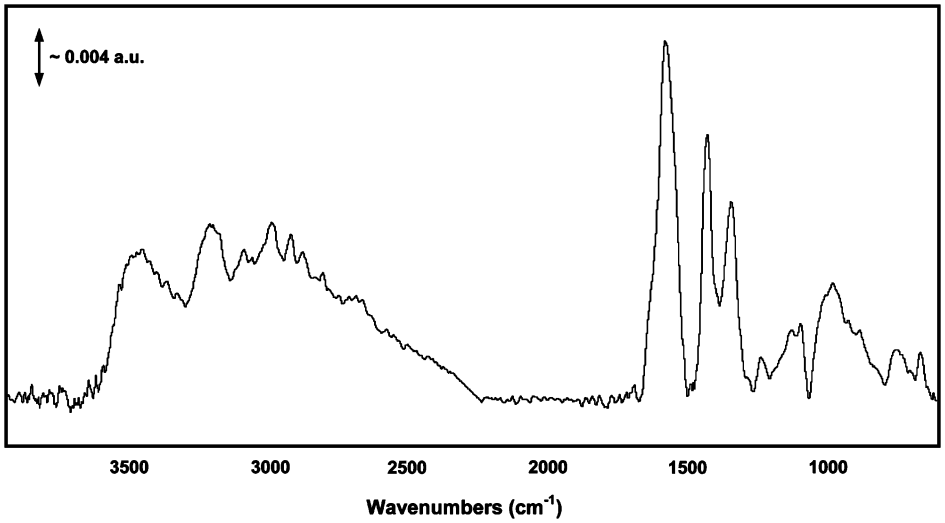

Figure 10. Transmission FTIR of Si-*g*-PtBA conversion with ethylenediamine (Si-*g*-PtBA→EDA).

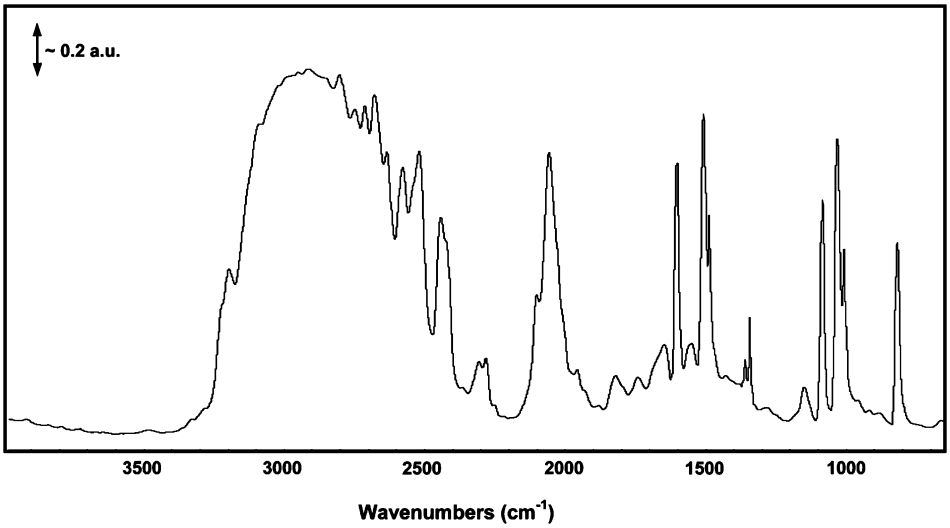

Figure 11. Transmission FTIR of Si-*g*-PtBA conversion with a 10-fold concentration increase of ethylenediamine (Si-*g*-PtBA→10× EDA).

in the N−H stretch region for the 12 h sample. Other researchers have found that the amide carbonyl decreased in wavenumber by up to 50 cm^{-1} due to hydrogen bonding between amide groups.[46] The amide II band (C−N stretch and N−H bend) is seen at ∼1566 cm^{-1} for both the 2 and 12 h samples.

Diamine Conversion Reactions on Si-*g*-PtBA. *FTIR Spectroscopy*. Since the reactions on the homopolymer PtBA were successful, the diamine conversions were conducted on Si-*g*-PtBA. As was the case with the Si-*g*-PtBA samples, ER-FTIR spectra could not be successfully obtained on these specimens. The transmission FTIR spectra shown below were obtained with a microscope ATR accessory as described previously. Even these transmission FTIR spectra were difficult to obtain due to low signal-to-noise ratios, absorbance from Si (which necessitated baseline corrections), and small scan area of the microscope ATR accessory. In Figure 8, the broad N−H stretch and amide B band for the amide groups from reaction of Si-*g*-PtBA with dimethylethylenediamine (Si-*g*-PtBA→DMEDA) is centered at ∼3300 cm^{-1}. The amide I and amide II bands can be seen at 1648 and 1542 cm^{-1}, respectively. Figure 9 shows a spectrum for Si-*g*-PtBA reacted with *N*-isopropylethylenediamine (Si-*g*-PtBA→*N*-isoEDA). A broad absorbance corresponding to the N−H stretching of the amide and amine groups can be seen at ∼3300 cm^{-1}. The hydrocarbon peaks are well-resolved in this sample (asymmetric CH_3 stretch at ∼2963 cm^{-1} asymmetric and symmetric CH_2 stretches at ∼2917 and 2850 cm^{-1}, respectively).[29,34] Peaks for the amide I and amide II are not well resolved in the region from ∼1500 to 1700 cm^{-1}. Strong peaks can be seen at ∼1260 and 801 cm^{-1} for the Si-$(CH_3)_2$ functionality and at ∼1097 and 1024 cm^{-1} for Si−O stretching.[34] The lack of strong N−H stretching and amide I and amide II peaks indicates an incomplete conversion of Si-*g*-PtBA to Si-*g*-PtBA→N-isoEDA.

The spectrum for Si-*g*-PtBA→EDA (ethylenediamine) is shown in Figure 10. The three absorbances that we expect for these molecules at high wavenumbers seem to be present at ∼3250, ∼3100, and ∼2950 cm^{-1} for the N−H stretch, amide B, and C−H stretching, respectively. There is also an additional band at ∼3500 cm^{-1}. While there are N−H stretch contributions from both the secondary amide groups and primary amines, it is possible this band can be attributed to the formation of a salt. The broad peak centered at ∼1620 cm^{-1} is likely a combination of C−O, C−N, and N−H absorbances from both the amide and amine groups.[29] An experiment was performed where a 10-fold excess of ethylenediamine was used and the spectrum is shown in Figure 11. The band centered at ∼2900 cm^{-1} is unique when compared to the other diamine reaction spectra. It is likely due to the asymmetric and symmetric stretching in the NH_3^+ group of the salt of our primary amine pendant group, which is normally a broad, strong band between

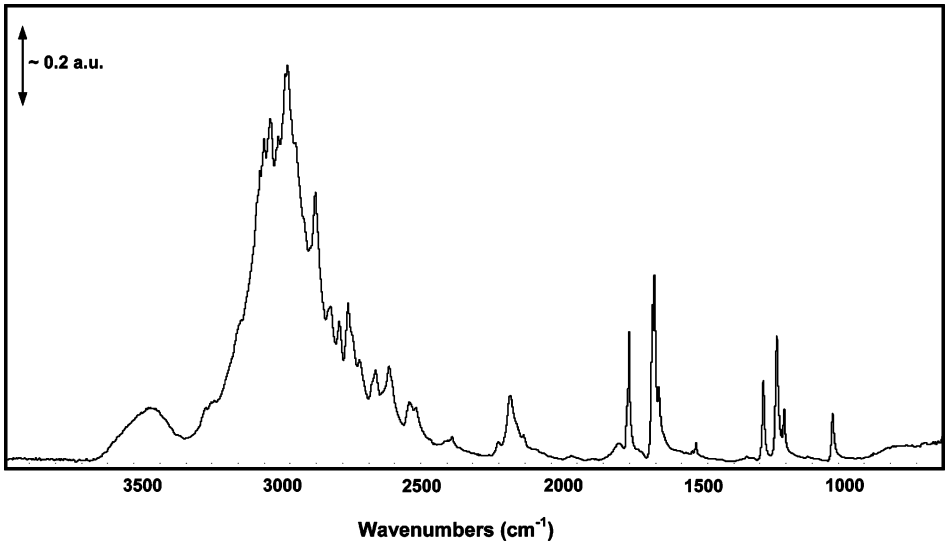

Figure 12. FTIR spectrum of ethylenediamine·2HCl salt from the HR Hummel Polymer and Additives spectral library.

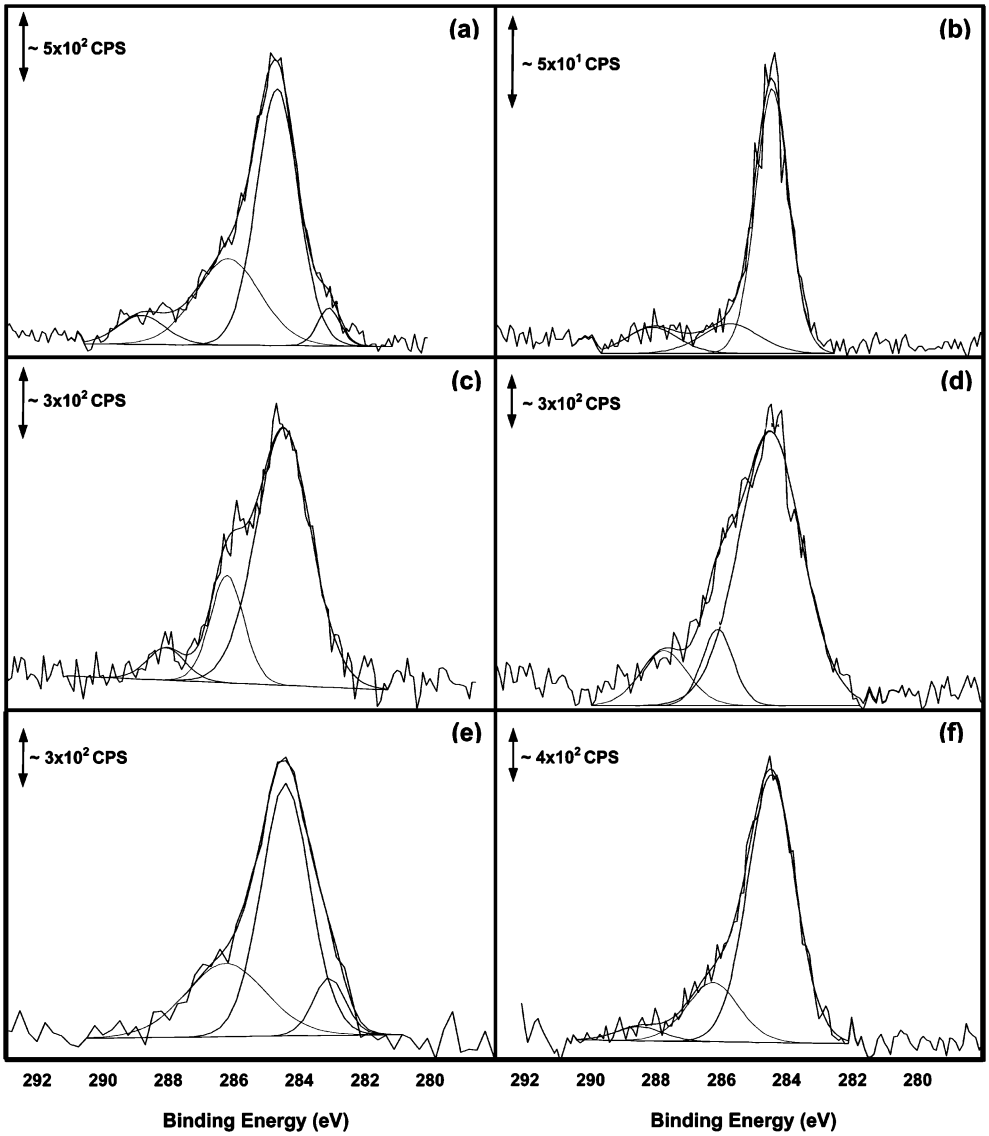

Figure 13. XPS C 1s high-resolution scans for (a) Si-*g*-PtBA→methylamine, (b) Si-*g*-PtBA→ethylenediamine, (c) Si-*g*-PtBA→dimethylethylenediamine, (d) Si-*g*-PtBA→diethylethylenediamine, (e) Si-*g*-PtBA→*N*-isopropylethylenediamine, and (f) Si-*g*-PtBA→diisopropylethylenediamine.

2800 and 3000 cm^{-1}.[29] A strong N−H stretch combination band present at ∼2060 cm^{-1} is also indicative of a primary amine salt.[29] The two bands at ∼1600 and 1510 cm^{-1} correspond to the asymmetric and symmetrical NH_3^+ N−H bending.[29] Indeed, the spectrum in Figure 11 has a peak pattern that is very similar to that of ethylenediamine·2HCl salt (shown in

Table 3. Atomic Composition and C/N Ratios for Si-*g*-PtBA→Diamine Samples from Survey XPS Scans[a]

sample		exptl	theor
Si-*g*-PtBA→MA	C	53.4 ± 2.2	61.5
	O	42.6 ± 2.8	20.5
	N	4.0 ± 0.6	18
	C/N	7.9 ± 1.0	3.4
Si-*g*-PtBA→EDA	C	63.2	57.7
	O	22.3	15.4
	N	14.5	26.9
	C/N	4.4	2.1
Si-*g*-PtBA→10× EDA	C	50.5 ± 6.9	57.7
	O	40.5 ± 10.2	15.4
	N	9.1 ± 3.5	26.9
	C/N	3.5 ± 1.2	2.1
Si-*g*-PtBA→DMEDA	C	56.7 ± 3.6, 44.6 ± 3.8	65.6
	O	37.8 ± 1.6, 48.0 ± 4.8	12.5
	N	5.5 ± 2.0, 7.5 ± 1.1	21.9
	C/N	6.6 ± 3.2, 3.5 ± 0.3	3.0
Si-*g*-PtBA→DEEDA	C	39.3	71.0
	O	57.0	10.5
	N	3.7	18.5
	C/N	10.6	3.8
Si-*g*-PtBA→diisopropyl EDA	C	38.5	75.0
	O	59.3	9.1
	N	2.2	15.9
	C/N	17.2	4.7
Si-*g*-PtBA→diisopropyl EDA	C	35.6 ± 2.9	68.6
	O	59.7 ± 4.9	11.4
	N	4.7 ± 2.4	20
	C/N	4.8 ± 1.7	3.4

[a]Samples with 95% confidence intervals were scanned at three different spots. The two sets of experimental data for Si-*g*-PtBA→DMEDA are for two different samples.

Figure 12) from the HR Hummel Polymer and Additives spectral library.

X-ray Photoelectron Spectroscopy. Because of the difficulty with using FTIR to confirm the chemistry within our relatively thin films on Si substrates, X-ray photoelectron spectroscopy (XPS) was used. Survey and high-resolution scans were made of the diamine converted Si-*g*-PtBA samples. The carbon high-resolution scans are shown in Figure 13 for the following samples: (a) Si-*g*-PtBA→methylamine (MA), (b) Si-*g*-PtBA→ethylenediamine (EDA), (c) Si-*g*-PtBA→dimethylethylenediamine (DMEDA), (d) Si-*g*-PtBA→diethylethylenediamine (DEEDA), (e) Si-*g*-PtBA→*N*-isopropylethylenediamine (*N*-isopropyl-EDA), and (f) Si-*g*-PtBA→diisopropylethylenediamine (diisopropyl-EDA). Except for Si-*g*-PtBA→MA, all of these diamines have two carbons between the amide and amine groups. Only Si-*g*-PtBA→MA and Si-*g*-PtBA→*N*-isopropylEDA (Figure 13a,e) have a peak present for Si−C at ∼283 eV. All of the Si-*g*-PtBA→diamine samples have peaks at ∼286.1 eV, which is shifted from the ∼285.5 eV peak found in Si-*g*-PtBA→PtBA (Figure 3). This shift is due to the increased content of *C*−N and (*C*═O)N. The small peak found at ∼288.3 eV in the Si-*g*-PtBA→diamine samples is likely from carboxylate anion ((*C*═O)O$^-$) functionality due to incomplete diamine conversion (since no remaining ester or acid content was observed in these samples with FTIR).

Atomic concentrations and C/N ratios from the survey scans of the Si-*g*-PtBA→diamine samples are shown in Table 3. The atomic concentrations were based only on carbon, oxygen, and nitrogen to provide a simpler basis for comparison of the samples. The survey scans also showed the presence of zinc (<3%) as a contaminant from the $ZnBr_2$ used in the diamine conversion reactions, and peaks for Si were seen for some of the Si-*g*-PtBA→diamine samples, but not for all. For all of the Si-*g*-PtBA→diamine samples the nitrogen atomic concentration was lower than the theoretical values, which were calculated for a pure layer of the polyamide formed. The low N content could be attributed to several factors. Even though no remaining ester or acid content was observed in these samples with FTIR, there could have been incomplete diamine conversion leaving a small fraction of carboxylate anions as discussed above. There is also the possibility of nitrogen loss from the XPS experiments themselves. Several researchers have found loss of 6−25% of nitrogen due to cleavage during XPS runs.[19,21,44] Since the measured oxygen content is also greater than theoretically expected, the silicon substrate is likely also being probed with the silicon oxide layer providing additional oxygen content. Additional possibilities for the presence of the excess oxygen include physisorbed reaction byproducts such as *tert*-butanol and water. This additional oxygen substantially decreased the measured atomic concentration (%) of nitrogen.

Conclusions

Amine-terminated silane self-assembled monolayers (SAMs) were deposited onto silicon (Si) wafers. The terminal amine reaction sites were used to graft end-functionalized PtBA. During the grafting reactions, some *tert*-butyl ester groups were hydrolyzed. In fact, the polymer can be converted to hydrolyzed poly(acrylate) (poly(acrylic acid), PAA). The pendant groups, whether acid, *tert*-butyl ester, or a mixture, were then converted to amide/amine functionalities using a novel diamine reaction. Each reaction step and the changes in surface properties were monitored with external reflectance FTIR (ER-FTIR), ellipsometry, and static water contact angle goniometry. Results showed that hydrolysis and diamine conversion reactions were successfully performed on both neat PtBA homopolymer and end-grafted PtBA (Si-*g*-PtBA). Among the diamines studied, FTIR and XPS analyses showed differences in the ability to completely convert the *tert*-butyl ester pendant groups, which is likely due to differences in diamine reactivity and steric hindrance. Ethylenediamine (EDA) and dimethylethylenediamine showed the highest conversion yields, although quantitative interpretation of the XPS data was difficult due to imperfect surface coverage of the SAM. Further study is needed to determine the optimal reaction conditions for complete conversion. In addition, the EDA conversion reaction was shown to form an amine salt, especially at higher EDA concentrations. The diamine reaction scheme reported here can be used to create polymers with amide and amine pendant group chemistries from acid and *tert*-butyl ester groups.

Acknowledgment. This work was supported by the ERC Program of the National Science Foundation under Award EEC-9731680 and by the Department of Education GAANN fellowship program. The authors thank Dr. Amol Janorkar and Dr. JoAn Hudson for the XPS measurements. Much appreciation is given to Kim Ivey in the School of Materials Science and Engineering at Clemson University for the transmission FTIR spectra.

References and Notes

(1) Hoffman, A. S. *Macromol. Symp.* **1996**, *101*, 443−454.
(2) Bergbreiter, D. *Prog. Polym. Sci.* **1994**, *19*, 529−560.
(3) Jones, R. A. L.; Lehnert, R. J.; Schonherr, H.; Vancso, J. *Polymer* **1999**, *40*, 525−530.
(4) Karim, A.; Satija, S. K.; Orts, W.; Ankner, J. F.; Majkraz, C. F.; Fetters, L. J. *Mater. Res. Soc. Symp. Proc. Polym./Inorg. Interfaces* **1993**, *304*, 149−154.
(5) Penn, L. S.; Hunter, T. F.; Lee, Y.; Quirk, R. P. *Macromolecules* **2000**, *33*, 1105−1107.

(6) Koutsos, V.; van der Vegte, E. W.; Hadziioannou, G. *Macromolecules* **1999**, *32*, 1233−1236.
(7) Takei, Y. G.; Aoki, T.; Sanui, K.; Ogata, N.; Sakurai, Y.; Okano, T. *Macromolecules* **1994**, *27*, 6163−6166.
(8) Karavia, V.; Deimede, V.; Kallitsis, J. K. *J. Macromol. Sci., Pure Appl. Chem.* **2004**, *41*, 115−131.
(9) Zdyrko, B.; Varshney, S. K.; Luzinov, I. *Langmuir* **2004**, *20*, 6727−6735.
(10) Boyes, S. G.; Mirous, B. K.; Brittain, W. J. *Polym. Prepr.* **2003**, *44*, 552−553. Boyes, S. G.; Akgun, B.; Brittain, W. J.; Foster, M. D. *Macromolecules* **2003**, *36*, 9539−9548.
(11) Lee, K.; Pan, F.; Carroll, G. T.; Turro, N. J.; Koberstein, J. T. *Langmuir* **2004**, *20*, 1812−1818.
(12) Wu, Y.; Limburg, D.; Wilkinson, D.; Vaal, M.; Hamilton, G. *Tetrahedron Lett.* **2000**, *41*, 2847−2849.
(13) Kaul, R.; Brouillette, Y.; Sajjadi, Z.; Hansford, K. A.; Lubell, W. D. *J. Org. Chem.* **2004**, *69*, 6131−6133.
(14) Walters, K. B.; Hirt, D. E. *Polymer* **2006**, *47*, 6567−6574.
(15) Urban, M. W. *Attenuated Total Reflectance Spectroscopy of Polymers: Theory and Practice*; American Chemical Society: Washington, DC, 1996.
(16) Silverstein, R.; Bassler, G.; Morrill, T. *Spectroscopic Identification of Organic Compounds*; John Wiley & Sons: New York, 1991; pp 103−124.
(17) Kupstov, A.; Zhizhin, G. *Handbook of Fourier Transform Raman and Infrared Spectra of Polymers*; Elsevier Science B.V.: Amsterdam, 1998; xxiv−xxvii.
(18) Bain, C. D.; Troughton, E. B.; Tao, Y.-T.; Evall, J.; Whitesides, G. M.; Nuzzo, R. G. *J. Am. Chem. Soc.* **1989**, *111*, 321−335.
(19) Fryxell, G. E.; Rieke, P. C.; Wood, L. L.; Engelhard, M. H.; Williford, R. E.; Graff, G. L.; Campbell, A. A.; Wiacek, R. J.; Lee, L.; Halverson, A. *Langmuir* **1996**, *12*, 5064−5075.
(20) Wieringa, R. H. Surface-Grafted Polyglutamate Films with Reaction-Induced Polar Order. Ph.D. Thesis, University of Groningen, The Netherlands, 2000, 19−35.
(21) Heiney, P. A.; Grüneburg, K.; Fang, J. *Langmuir* **2000**, *16*, 2651−2657.
(22) Plueddemann, E. P. *Silane Coupling Agents*; Plenum Press: New York, 1982.
(23) Tredgold, R. H. *Order in Thin Organic Films*; Cambridge University Press: Cambridge, 1994; pp 128−124.
(24) Duchet, J.; Chabert, B.; Chapel, J. P.; Gérard, J. F.; Chovelon, J. M.; Jaffrezic-Renault, N. *Langmuir* **1997**, *13*, 2271−2278.
(25) Jeon, N. J.; Finnie, K.; Branshaw, K.; Nuzzo, R. G. *Langmuir* **1997**, *13*, 3382−3391.
(26) Kurth, D. G.; Bein, T. *Langmuir* **1993**, *9*, 2965−2973.
(27) Moon, J. H.; Shin, J. W.; Kim, S. Y.; Park, J. W. *Langmuuir* **1996**, *12*, 4621−4624.
(28) Vallant, T.; Brunner, H.; Mayer, U.; Hoffman, H. *J. Phys. Chem. B* **1998**, *102*, 7190−7197.
(29) Silverstein, R. M.; Bassler, G. C.; Morrill, T. C. *Spectrometric Identification of Organic Compounds*; John Wiley & Sons: New York, 1991.
(30) Kuptsov, A. H.; Zhizhin, G. N. *Handbook of Fourier Transform Raman and Infrared Spectra of Polymers*; Elsevier: Amsterdam, 1998.
(31) Shreedhara, Murthy, S.; Blitz, J. P.; Leyden, D. E. *Anal. Chem.* **1986**, *58*, 3167−3172.
(32) Shreedhara, R. S.; Leyden, D. E. *Anal. Chem.* **1986**, *58*, 1228−1233.
(33) Coates, J. Interpretation of Infrared Spectra, A Practical Approach. In *Encyclopedia of Analytical Chemistry*; Meyers, R. A., Ed.; John Wiley and Sons, Ltd.: New York, 2000.
(34) Bellamy, L. J. *The Infra-red Spectra of Complex Molecules*; Methuen & Co., Ltd.: London, 1958.
(35) Mengel, C.; Esker, A. R.; Meyer, W. H.; Wegner, G. *Langmuir* **2002**, *18*, 6365−6372.
(36) Nakayama, Y.; Matsuda, T. *Macromolecules* **1996**, *29*, 8622−8630.
(37) Wang, T.; Kang, E. T.; Neoh, K. G.; Tan, K. L.; Liaw, D. J. *Langmuir* **1998**, *14*, 921−927.
(38) Ista, L. K.; Mendez, S.; Perez-Luna, V. H.; Lopez, G. P. *Langmuir* **2001**, *17*, 2552−2555.
(39) Clark, D. T.; Thomas, H. R. *J. Polym. Sci., Polym. Chem. Ed.* **1978**, *16*, 791−820.
(40) Lee, Y. M.; Shim, J. K. *Polymer* **1997**, *38*, 1227−1232.
(41) Chang, G. S.; Jung, S. M.; Lee, Y. S.; Choi, I. S.; Whang, C. N.; Woo, J. J.; Lee, Y. P. *J. Appl. Phys.* **1997**, *81*, 135−138.
(42) Pan, F.; Wang, P.; Lee, K.; Wu, A.; Turro, N. J.; Koberstein, J. T. *Langmuir* **2005**, *21*, 3605−3612.
(43) Balachander, N.; Sukenik, C. *Langmuir* **1990**, *6*, 1621−1627.
(44) Heise, A.; Stamm, M.; Rauscher, M.; Duschner, H.; Menzel, H. *Thin Solid Films* **1998**, *327−329*, 199−203.
(45) Lee, I.; Wool, R. P. *Thin Solid Films* **2000**, *379*, 94−100.
(46) Kong, X.; Kawai, T.; Abe, J.; Iyoda, T. *Macromolecules* **2001**, *34*, 1837−1844.
(47) Frauenfelder, H. *Vibrations* in *Physics of Proteins*; Chan, S., Austin, R., Eds. [hhtp://wwwphy.princeton.edu/∼austin/hf_book/hfbook.html].
(48) Grdadolnik, J. *Internet J. Vib. Spectrosc.* [www.ijvs.com] **2004**, *6*, 6.
(49) Cho, S. H.; Jhon, M. S.; Yuk, S. H.; Lee, H. B. *J. Polym. Sci., Part B* **1997**, *35*, 595−598.

MA0700882